Article:
Avgoustou, P., Jailani, A.B.A., Zirimwabagabo, J.-O. et al. (15 more authors) (2020) Discovery of a first-in-class potent small molecule antagonist against the adrenomedullin-2 receptor. ACS Pharmacology & Translational Science. ISSN 2575-9108

https://doi.org/10.1021/acsptsci.0c00032

Title: Discovery of a first-in-class potent small molecule antagonist against the Adrenomedullin-2 receptor

Paris Avgoustou[1^], Ameera B A Jailani[1^], Jean-Olivier Zirimwabagabo[2^], Matthew J Tozer[3], Karl R Gibson[4], Paul A Glossop[4], James EJ Mills[4], Rod A Porter[5], Paul Blaney[6], Peter J Bungay[7], Ning Wang[1], Alice P Shaw[1], Kamilla J A Bigos[1], Joseph L Holmes[1], Jessica I Warrington[1], Timothy M Skerry[1ǂ*], Joseph PA Harrity[2ǂ] and Gareth O Richards[1ǂ].

1. Department of Oncology and Metabolism, University of Sheffield, UK
2. Department of Chemistry, University of Sheffield, UK
3. Matt Tozer Consultancy, Cambridge, UK
4. Sandexis Medicinal Chemistry Ltd, Sandwich, Kent, UK
5. Rod Porter Consultancy, Ashwell, Hertfordshire, UK
6. Concept Life Sciences, High Peak UK
7. Sympetrus Ltd., Bishop's Stortford, Hertfordshire, UK

^ ǂ These authors contributed equally to the work

*Correspondence to T M Skerry
Email: t.skerry@sheffield.ac.uk

Keywords
Adrenomedullin; AM_1 receptor, AM_2 receptor, G protein-coupled receptor, receptor activity-modifying protein

Abstract

The hormone adrenomedullin has both physiological and pathological roles in biology. As a potent vasodilator, adrenomedullin is critically important in regulation of blood pressure, but it also has several roles in disease, of which its actions in cancer are becoming recognized to have clinical importance. Reduced circulating adrenomedullin causes increased blood pressure but also reduces tumor progression, so drugs blocking all effects of adrenomedullin would be unacceptable clinically. However, there are two distinct receptors for adrenomedullin, each comprising the same G protein-coupled receptor (GPCR), the calcitonin receptor-like receptor (CLR), together with a different accessory protein known as a receptor activity-modifying protein (RAMP). CLR with RAMP2 forms an adrenomedullin-1 receptor and CLR with RAMP3 forms an adrenomedullin-2 receptor. Recent research suggests that selective blockade of adrenomedullin-2 receptors would be a valuable therapeutically. Here we describe the design, synthesis and characterization of potent small molecule adrenomedullin-2 receptor antagonists with 1,000-fold selectivity over the adrenomedullin-1 receptor, although retaining activity against the CGRP receptor. These molecules have clear effects on markers of pancreatic cancer progression *in vitro*, drug-like pharmacokinetic properties and inhibit xenograft tumor growth and extend life in a mouse model of pancreatic cancer. Taken together, our data support the promise of a new class of anti-cancer therapeutics as well as improved understanding of the pharmacology of the adrenomedullin receptors and other GPCR/RAMP heteromers.

Introduction

Development of new therapeutic agents requires insights into the fundamental biology of target systems and ability to modulate the target in disease without causing deleterious off-target effects elsewhere. Adrenomedullin (AM) is a potent vasodilator which acts to control blood pressure by regulating functions including vasomotor tone [1] and glomerular filtration rate [2]. Soon after the discovery of the hormone, profound increases in circulating AM were shown to be associated with catastrophic low blood pressure in patients with sepsis, who suffered consequent reduced organ perfusion and, in many instances, death [3-5]. AM is also expressed by most tumors [6], leading to high serum AM levels [7] in patients. AM-mediated actions include increased tumor growth and markers of tumor progression [8] as well as being implicated in metastatic spread [9]. As a target in cancer, AM is therefore compromised because reduction in circulating levels or blockade of all its actions would cause hypertension. However, there are two receptors for AM, each a heteromeric complex of the calcitonin receptor-like receptor (CLR, a Family B GPCR) to which ligand selectivity is conferred by association with one of the 3 human receptor activity-modifying proteins (RAMPs) [10, 11] (Figure 1a). While RAMPs have previously been studied primarily in context of Family B GPCRs, RAMPs have also been shown to have coevolved with many other GPCR families [12, 13]. All three CLR/RAMP complexes have distinct pharmacological and physiological properties which are driven by the subtype of RAMP with which CLR interacts [14]. Specifically, the CLR/RAMP1 heteromer is a receptor for calcitonin gene-related peptide (CGRP), a neuropeptide implicated in pain sensing [14] and small molecule antagonists of the CGRP receptor have been the subject of considerable research [15-17]. The CLR with RAMP2 forms an AM_1 receptor while the CLR with RAMP3 forms an AM_2 receptor [11, 14, 18]. While the AM_1 receptor is essential for physiological processes including cardiovascular health [19], aberrant AM_2 receptor signalling can result in cancer-promoting pathways [7, 20-24]. In the AM receptors, despite the relatively modest structural differences, their physiological roles are becoming more distinctly defined.

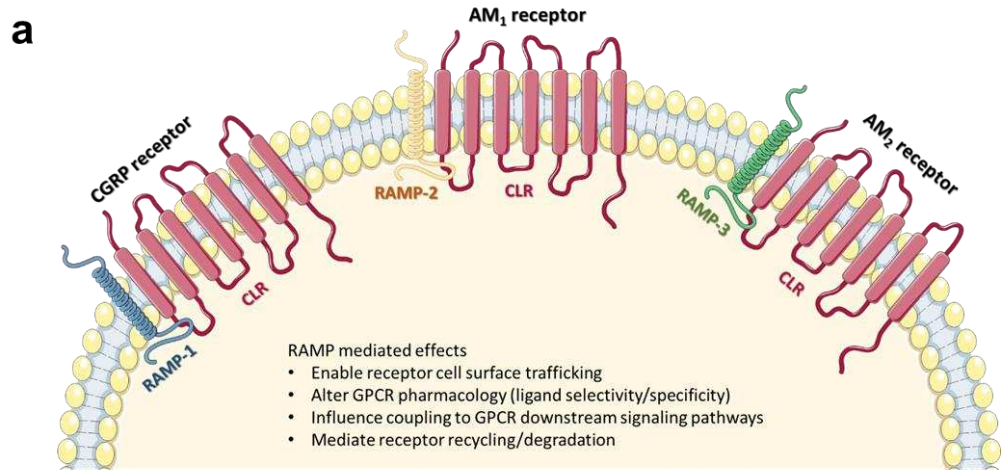

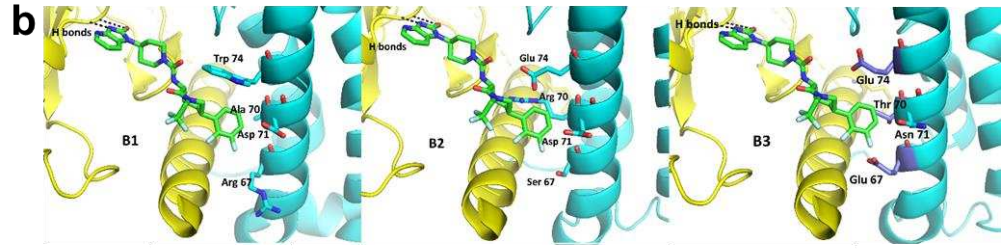

Protein	Protein residue number (PDB codes: 3N7R, 3AQF)			
	67	70	71	74
RAMP1	Arg	Ala	Asp	Trp
RAMP2	Ser	Arg	Asp	Glu
RAMP3	Glu	Thr	Asn	Glu

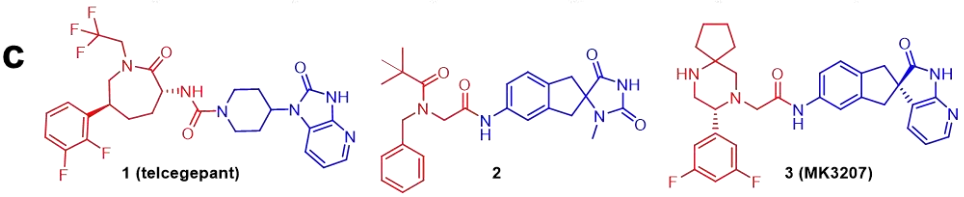

Figure 1: Cellular role of CLR and RAMP complexes and their interactions with small molecules (**a**) Interaction of CLR receptor with a different RAMP leads to three CLR/RAMP receptor complexes with distinct pharmacological and physiological properties. (**b**) Models of CLR/RAMP complexes with **1 (telcagepant),** based on crystal structures of CGRP and AM_1 receptors (PDB code: 3N7R and 3AQF respectively). CLR is rendered in yellow and RAMP in cyan in each of CLR/RAMP1 (B1), CLR/RAMP2 (B2), CLR/RAMP3 (B3). RAMP residues (at **1** binding site) that differ across RAMP1/RAMP2/RAMP3 are highlighted and labelled. (**c**) In order to design analogues with increased potency against AM_2 receptor, the CLR binding motifs (blue) were

relatively conserved whereas the RAMP binding motifs (red) were used as scaffolds for basic groups to interact with Glu residues on RAMP3.

In gene knockout mouse studies, deletion of the gene for the AM ligand leads to intrauterine death at mid-gestation, due to a vascular and lymphatic phenotype known as hydrops fetalis [25]. That phenotype is copied exactly by deletion of the CLR, which prevents the formation of both AM_1 and AM_2 receptors [26]. Interestingly though, RAMP2 null mice have the same phenotype [27], with the same embryonic lethality and even heterozygotes exhibit significant pathology due to haploid insufficiency. In stark contrast, RAMP3 null mice are viable and healthy and even have some advantageous phenotypic characteristics [19] some of which may be replicated in humans with single nucleotide polymorphisms in RAMP3 [28]. Knockout experiments in mice are hard to interpret with precision as RAMPs interact not only with CLR but a number of other receptors including calcitonin receptors (CTR) where heteromers are amylin receptors. However, until very recently, no agonists or antagonists were available that provided useful discrimination between RAMP2 and RAMP3[29].

The published crystal structures of CLR/RAMP1 (CGRP receptor) and CLR/RAMP2 (AM_1 receptor) heteromers bound to truncated peptide antagonists $CGRP_{27-37}$ and AM_{25-52} respectively, give insights into association of ligands with CLR/RAMP receptors [30, 31]. A hydrophobic patch and a pocket that are separated by the CLR Trp72 shelf (Trp72 bulge) [30, 31] are established features. The hydrophobic patch is a region of aromatic residues in CLR: Trp72, Phe92, Phe95 and Tyr124 [30]. The pocket is larger and incorporates residues of both components: Asp70, Trp72, Gly71, Trp121, Thr122 and Tyr124 of CLR with Trp74, Trp84 and Pro85 in RAMP1 or Arg97, Glu101, Glu105, Phe111 Pro112 in RAMP2 [30]. Trp84 in RAMP1 corresponds to the same position as Glu101 in RAMP2. Both residues were previously identified as key residues for CGRP [32] and AM [33] function. These data suggest the presence of a β-turn on both CGRP and AM peptides that enables them to occupy their respective binding pockets and modulates interactions with CLR and RAMP residues. More specifically, via its Phe37 phenyl ring, CGRP interacts with CLR residues Gly71 and Trp72 and RAMP1 residue Trp84 [30]. CGRP binds almost entirely on CLR and

makes only one critical contact with RAMP1 extracellular domain (at residue Trp84) which also includes a hydrophobic interaction with CLR residue Phe37 [30]. Hydrogen bonds are formed between CGRP residue Val32 and the Trp72 bulge of CLR and a main-chain to side-chain connection is made between CGRP Thr30 and CLR loop 3 Asp94 residues [30].

Similarly, AM residues Tyr52 and Lys46 interact with residues Arg97, Glu101 and Glu105 on RAMP2 [30]. An extension of a single helical turn allows AM Lys46 to contact the Trp72 bulge and AM Pro43 and Ala42 to interact with the patch [30]. The equivalent residue on RAMP1 (Trp74) is unable to interact with AM [30]. This was explained by absence of a Glu residue at position 74 of RAMP1 that discourages AM interaction [30]. The importance of residues Glu101 and Phe111 on RAMP2 was previously shown through mutagenesis studies [33]. Recent studies, including the recently published cryo-EM structures of the whole CGRP, AM_1 and AM_2 receptors, have given a deeper understanding to these receptor complexes and their mechanisms of activation [34-36].

Small-molecule CGRP receptor antagonists (olcegepant, telcagepant, MK-3207, ubrogepant and rimegepant) have been developed [37]. Some have reached the clinic, notably ubrogepant (Ubrelvy, NCT02828020) and rimegepant (Nurtec ODT, NCT03461757). This indicates the potential for developing selective antagonists for other CLR/RAMP heteromers (the AM_1 and AM_2 receptors) by exploiting the key residue differences between RAMPs [38-42]. Structural relationship studies within the gepant family of CGRP receptor antagonists have identified the presence of three important interactive regions in CLR/RAMP heteromers within the CGRP receptor antagonists – the CLR binding region, the interface region that binds close to the Trp72 bulge and the CLR/RAMP1 binding region that interacts with the CLR/RAMP-1 hydrophobic patch – that facilitate their binding and selectivity [43].

While previous efforts to manipulate AM receptor function have been to target isolated components of the system – the AM ligand or receptor components (CLR, RAMP2 or RAMP3) – using antibodies or peptide antagonists, we have developed small molecule antagonists that

specifically target AM signalling through AM_2 receptor. Recently, small molecule positive allosteric modulators against CLR-based receptor complexes have been identified, which are not active on other class B GPCRs including the closely related CTR [44]. Our approach enables AM to continue physiological signalling through AM_1 receptors, decreasing possibilities of side effects resulting from this therapeutic strategy. AM and RAMP3 have been shown to mediate pro-tumoral processes in various cancers [7, 20-23], including pancreatic cancer [24, 45]. A recent publication has also shown the involvement of AM/RAMP3 system (but not AM/RAMP2) in liver metastasis of pancreatic cancer through modification of cancer-associated fibroblasts [45]. Since pancreatic cancer is currently an unmet clinical need for life-extending therapy, we have selected that as a therapeutic target.

Results and discussion

Design of potent selective small molecule AM_2 receptor antagonists

As CGRP, AM_1 and AM_2 receptors comprise the same CLR component but a different RAMP, we envisaged that improvements in potency and selectivity towards AM_2 receptors would be gained by exploiting and optimizing specific interactions with RAMP3 that would be unlikely to be replicated with RAMP1 or RAMP2. In order to design analogues with increased potency against the AM_2 receptor, we inspected the sequences of RAMPs 1, 2 and 3 and their relationship to the binding site for the known small-molecule CGRP receptor antagonists.

Figure 1B1 shows the published structure [30] of telcagepant **1** (green) – a CGRP receptor antagonist – crystallized in the extracellular domains of the CLR (yellow) / RAMP1 (cyan) heteromer (PDB code: 3N7R). Figures 1B2 and 1B3 show the same structure (**1**) with RAMP2 and RAMP3 residues changes respectively highlighted. The RAMP3 amino acid residues which differ from the RAMP1 sequence at the small molecule antagonist binding site are highlighted, specifically Glu74 (Trp in RAMP1), Thr70 (Ala in RAMP1) and Glu67 (Arg in RAMP1). We hypothesized that the acidic glutamate residues, which are present in RAMP3 but not RAMP1 provide an opportunity to target RAMP3 by the introduction of basic centres in a small molecule.

Furthermore, while Glu74 is common to RAMP2, that protein has a large Arg residue at position 70, which effectively occludes the small molecule antagonist binding site as it exists in CLR/RAMP1 or CLR/RAMP3 receptors. We surmised that introduction of basic centres to small molecule CGRP antagonists could improve interactions with glutamate residues in RAMP3 (AM_2 receptor) without an expectation of potent interactions with RAMP2 (AM_1 receptor).

The majority of CGRP receptor small molecule antagonists showed minimal or no activity against AM_1 and AM_2 receptors[37]. However, a search of the literature highlighted two CGRP receptor antagonists with encouraging activity against AM_2 receptor – compounds **3** (MK-3207) [46] and **2** [47] (pIC_{50} = 6.20 and 5.97 respectively for AM_2 receptor respectively, determined in house). Comparison with the chemical structure of the more selective CGRP antagonist telcagepant (**1**) allowed us to highlight areas of each molecule which bind to CLR (blue) and RAMP (red) proteins (Figure 1c). In the CGRP receptor antagonist field, the CLR binding motifs have been relatively conserved. That led us to the idea that the close relationship between the CGRP and AM_2 receptors and the combination of these well-established CLR-binders with a head group designed to maximize preferential binding to RAMP3 over both RAMP1 and RAMP2 could deliver AM_2 receptor-preferring molecules. To this end, we targeted the red portions in Figure 1c as scaffolds for basic groups to interact with the glutamyl residues on RAMP3.

Identification of small molecule AM_2 receptor selective/potent antagonists

Beginning with **2** (pIC_{50} = 5.97 for AM_2 and 7.77 for CGRP receptors, Figure 2a), introduction of the CLR binding motif from **3** afforded compound **5** (pIC_{50} = 6.55 for AM_2 and 8.31 for CGRP receptors, Figure 2a) which showed an increase in potency at both AM_2 and CGRP receptors. Introduction of a benzylic amine into **2** afforded **4** (pIC_{50} = 6.44 for AM_2 and 6.57 for CGRP receptors, Figure 2a) which showed a similar improvement in potency at AM_2 receptor as **5** relative to **2** but balanced activity against CGRP receptor. A combination of these changes led to **6** (pIC_{50} = 8.31 for AM_2 and 8.09 for CGRP receptors, Figure 2a) and gave the first dramatic improvement in AM_2 activity. Subsequent addition of a small substituent to the benzylic amine led

to the discovery of **7** (pIC_{50} = 9.16 for AM_2 and 8.38 for CGRP receptors, Figure 2a). Compound **7** is the first highly potent and selective AM_2 receptor small molecule antagonist, providing a 1000-fold increase in potency relative to commercially available CGRP antagonists (such as **3**). Further analysis showed significant pharmacological differences between the two enantiomeric forms of **7** (racemate), with compound **8** ((*R*)-enantiomer, pIC_{50} = 9.21 for AM_2 and 9.07 for CGRP receptors, Figure 2a) showing higher affinity than the (*S*)-enantiomer (**9**, pIC_{50} = 7.16 for AM_2 and 7.09 for CGRP receptors, Figure 2a). These hits were then screened against the AM_1 receptor. As we predicted, lead compounds showed significant selectivity (more than 100-fold) for AM_2 and CGRP receptors over the AM_1 receptor (Figure 2a). This selectivity was maintained for other members of the calcitonin family of receptors (CTR, AMY_1 and AMY_3, Figure 2b, Figure S1 and Table S3). We believe the activity profile of our compounds is consistent with the proposed unfavourable steric clash with Arg70 of RAMP2 with tolerance of the conformationally flexible benzylic amine by the CGRP receptor through either ionic interaction with Asp71 or exposure to solvent. To determine if AM_2 receptor antagonists was able to inhibit AM-induced cAMP production in native cells, **7** and its enantiomers (**8** and **9**) were tested in a human pancreatic cancer cell line CFPAC-1. Similar to results in the over-expressing cell lines (Figure 2a), **7** (pIC_{50} = 9.33, Figure 2c) and its (*R*)-enantiomer (**8**, pIC_{50} = 8.96, Figure 2c) were able to inhibit AM-induced cAMP production 100-fold more potently than its (*S*)-enantiomer (**9**, pIC_{50} = 7.02, Figure 2c). In addition to their effect in human cells, AM_2 receptor antagonists were able to inhibit AM-induced cAMP production in other species including mouse and dog (Figure S2). Additionally, lead compounds were tested in a mouse cell line (178-2 BMA cells) to determine the potential effect of AM_2 receptor antagonists on host cells in an *in vivo* tumor model. Interestingly, the activity of lead compounds on mouse cells were 2- to 100-fold less than in human cells (Figure 2c). Modelling showed no obvious residue differences at the key binding site in RAMP3 between the species, however subtle conformational variations may be the cause of observed differences in potency.

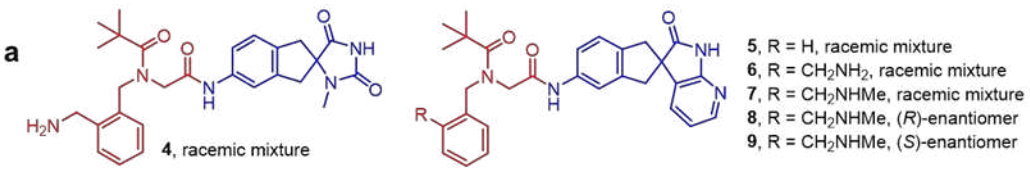

Receptor	Compound 2	Compound 4	Compound 5	Compound 6	Compound 7	Compound 8	Compound 9
	Mean pIC_{50} ± SEM						
CGRP	7.77±0.10[a]	6.57±0.09	8.31 ±0.09[a]	8.09±0.08	8.38±0.07[a]	9.07±0.09	7.09±0.08
AM_1	5.43±0.23	6.15±0.15	5.11±0.16[a]	5.63±0.18[a]	5.58±0.08[a]	5.86±0.11[a]	5.32±0.19[a]
AM_2	5.97±0.19	6.44±0.11	6.55±0.09	8.31±0.16	9.16±0.09	9.21±0.12	7.16±0.11

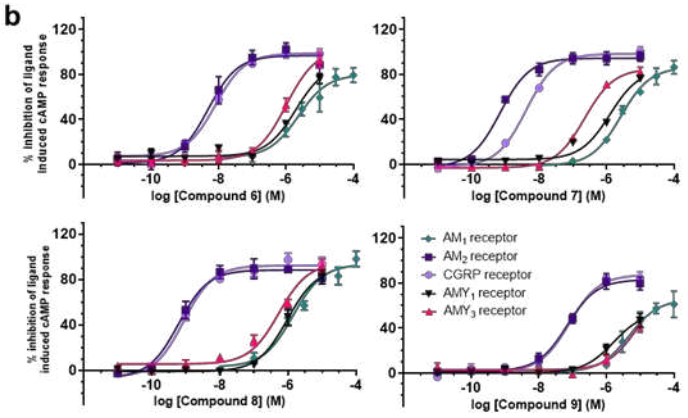

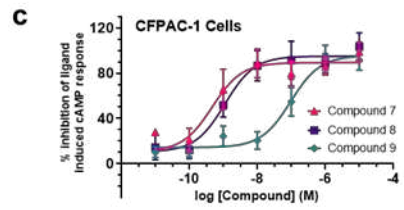

Compound	Human CFPAC-1 Cells Mean pIC_{50} ± SEM	Mouse 178-2 BMA Cells Mean pIC_{50} ± SEM
7	9.33±0.40	7.37±0.10[a]
8	8.96±0.28	8.40±0.18[a]
9	7.02±0.22	nd

Figure 2: **Activity and selectivity of early lead compound 6, current lead compound 7 and its enantiomers (8 and 9) in CLR/RAMP overexpressing and native (human and mouse) cell lines.** (**a**) Primary screening was performed by measuring the ability of small molecules in inhibiting cAMP production in cell lines over-expressing each receptor complex. Early lead compound **6** was equipotent in inhibiting both CGRP and AM_2 receptors. Current lead compound **7** racemate was the first small molecule antagonist with even modest selectivity for AM_2 receptor over CGRP receptor (the difference was significant and 7-10-fold). (*R)*-enantiomer **8** is 100-fold more potent in inhibiting cAMP in both CGRP and AM_2 receptors, compared to (*S)*-enantiomer **9**. Lead compounds are significantly more selective for CGRP and AM_2 receptors over other members of the calcitonin family of receptors (AM_1, AMY_1 and AMY_3 receptors). Data are from at least three independent experiments and presented as mean±SEM. Curves are representative and do not include all data points (**b**) Graphical representation of results in (**a**). (**c**) Activity of current lead compound **7** and its enantiomers (**8** and **9**) in inhibiting AM-induced cAMP production were also tested in human pancreatic cancer cell line CFPAC-1 and mouse prostate cancer cell line 178-2 BMA. The activity of lead compounds on human CFPAC-1 cells were similar to that in overexpressing cells (**a, b**), whereas the activity on mouse 178-2 BMA were 2- to 100-fold less. [a]$p<0.05$ by unpaired t-test compared to the pIC50 of each compound on the AM_2 receptor cells.

AM_2 receptor antagonists showed ADME properties suitable for further optimization as drug-like molecules

In vitro studies on **7** and the more potent single enantiomer **8** were performed in order to characterize their ADME and physicochemical properties (Table 1). Compounds **7** and **8** were determined to be moderately lipophilic with $logD_{7.4}$ of 1.58 and 1.59, respectively and possessed low aqueous solubility at pH 7.4 between 86.3 and 199 µM. Intrinsic clearance (CL_{int}) via metabolism measured in liver microsomes from human (21-22 µl/min/mg protein), rat (14-16 µl/min/mg protein) and mouse (22 µl/min/mg protein) was at a level low enough to support the use of the compounds in further *in vivo* pharmacokinetic and efficacy studies. Scaling of human liver microsomes CL_{int} of **8** using the well-stirred model of hepatic metabolic clearance[48, 49] predicted blood CL of 4.7 ml/min/kg in human, a relatively low fraction of hepatic blood flow (21 ml/min/kg). Compounds **7** and **8** displayed moderate binding to plasma proteins with unbound fractions of 17.6% in rat (**7** and **8**), 8.7% in mouse (**7**) and 22.9 (**7**) and 28.6 (**8**) in human. The results of these early ADME screening data indicate that compounds 7 and 8 are suitable lead compounds for further optimisation as potential drug molecules.

The inhibition profiles of **7** and **8** against several cytochrome P450 enzymes (CYPs) were also determined (Table 1). Both compounds were inhibitors of CYPs 2D6 (IC_{50} of **7** = 3.64 µM; **8** = 1.60 µM) and 3A4 (IC_{50} of **7** = 2.35 µM; **8** = 7.3 µM) but were less potent against 1A2 (IC_{50} >50 µM), 2C9 (IC_{50} of **7** = 34.15 µM; **8** > 50 µM) and 2C19 (IC_{50} of **7** = 26.19 µM; **8** >50µM). These data show that compounds **7** and **8** possess modest potency as inhibitors of major drug-metabolising CYPs and that this chemical series is capable of being optimised for low risk of interaction with drugs metabolised by CYPs. Both compounds were also assessed for inhibition of hERG potassium channel currents as a routine indicator of risk of cardiac arrhythmia resulting from hERG inhibition [50]. Both were found to have IC_{50} >30 µM, indicating low risk.

The pharmacokinetic characteristics of **7** and **8** in rodents were examined following intravenous (i.v.) and oral administration by gavage (p.o.). In rats (Table 2) CL following i.v. administration of **7**

(2.66 mg/kg) and **8** (2.0 mg/kg) was similar, and high in relation to hepatic blood flow at 73.6 ml/min/kg (**7**) and 62.6 ml/min/kg (**8**). The moderate to high volume of distribution of **7** (8.0 L/kg) and **8** (16.8 L/kg) resulted in terminal half-lives of the compounds between 3.0 and 5.2 h. Bioavailability following p.o. administration of **7** (13.3 mg/kg) was only 1%. *In vitro* permeability data obtained in Caco-2 cell monolayers (Table 1) demonstrated low permeability and high efflux ratios that are consistent with poor absorption in the gut. However, the high CL observed, which indicates high hepatic extraction, would also limit oral bioavailability of **7** and **8**.

In support of experiments aimed at testing the effects of compounds on tumour growth in mice, comparison of compound exposure following i.v. and intraperitoneal (i.p.) administration of **7** as a solution in 50% PEG E 400 indicated high bioavailability of 83% via the i.p. route at a dose of 9.46 mg/kg (Table 2). T_{max} was 0.083-0.25 h with a C_{max} of 1333 ng/mL, equivalent to an unbound plasma concentration of 221 nM (Table 2). Administration of **8** at 9.69mg/kg via the i.p. route as a solution in 10% DMSO/50% solutol displayed a slightly higher C_{max} (1647 ng/mL, equivalent to unbound 273 nM, assuming an unbound fraction equal to that of **7**), similar t_{max} (0.083-0.25 h) (Table 2) but shorter half-life of 1.3 h (rat i.v. data, Table 2). Whilst the plasma concentration profiles of the racemic mixture (**7**) and active enantiomer (**8**) differed in these experiments (Figure S3), the difference is likely to have resulted from the suspension and solution formulations used, leading to slow and faster absorption, respectively, from the site of injection. Overall, these data demonstrate that concentrations of **7** and **8** can be attained via the i.p. route in mice that are relevant to AM_2 pharmacological potency.

Property		Units	species	7	8
molecular weight		Da	-	525.65	525.65
logD, pH 7.4		-	-	1.58	1.59
solubility, pH 7.4		µM	-	86.3	199
CL_{int}, liver microsomes		µl/min/mg protein	human	20.6±1.3	22.5±0.33
			Rat	13.6±1.2	16.4±1.32
			mouse	22±0.9	N.D.
plasma protein binding		%unbound fraction	human	22.9±0.8	26.8±0.4
			Rat	17.6±0.3	17.6±0.4
			mouse	8.7±0.9	N.D.
plasma stability t½		Min	human	>120	N.D.
Caco-2 permeability A:B		$cms^{-1} \times 10^{-6}$	human	<0.01	<0.01
Caco-2 permeability B:A		$cms^{-1} \times 10^{-6}$	human	9.11±0.62	8.38±0.43
CYP inhibition	**1A2**	µM	human	>50	>50
	2C9			34.15±1.01	>50
	2C19			26.19±0.5	>50
	2D6			3.64±1.5	1.6±0.15
	3A4			2.35±0.9	7.3±1.2
hERG currents		µM	-	>30	>30

Table 1: **ADME properties of lead compound 7 and 8**

hERG potassium channel currents were determined in quadruplicate, Caco-2 permeability, plasma protein binding, CYP inhibition and liver microsomal CL_{int} in triplicate and solubility, logD, plasma stability and were determined in duplicate. Data are presented as mean ± SD.

dose route	Parameter	7	8
Rat Pharmacokinetics			
i.v.	dose (mg/kg)	2.66	2.0
	plasma CL (mL/min/kg)	77.0±5.1	65.6±7.4
	Vss (L/kg)	8.0±2.7	16.8±1.7
	terminal t½ (h)	3.0±2.0	5.2±0.07
p.o.	dose (mg/kg)	13.3	N.D.
	F (%)	1.0	N.D.
Mouse Pharmacokinetics			
i.v.	dose (mg/kg)	2.06	N.D.
	plasma CL (mL/min/kg)	37.8±8.9	N.D.
	Vss (L/kg)	3.2±5.1	N.D.
	terminal t½ (h)	1.3±0.2	N.D.
i.p.	dose (mg/kg)	9.46	9.69
	Tmax (h)	0.083 - 0.25	0.083- 0.25
	unbound Cmax (nM)	221±28	273±37
	F (%)	83	N.D.

Table 2: Pharmacokinetic characteristics of lead compounds 7 and 8

Data are presented as mean ± SD for determinations in 3 animals. Bioavailability (F) was calculated from mean AUC according to: F = (AUC,p.o./dose,p.o.) / (AUC,i.v./dose,i.v.).

AM_2 receptor antagonists inhibit pancreatic tumor growth *in vitro* and *in vivo* in mice

As there are many well-documented pathological functions of AM and the AM_2 receptor in cancer, we used cancer cell and animal models to characterize our lead compounds. A panel of human pancreatic cancer cells (AsPC-1, Capan-2, CFPAC-1, HPAF-II and Panc10.05) have been shown to express AM, CLR and RAMPs mRNA (Table S4). Lead AM_2 receptor antagonists were subsequently tested on CFPAC-1 (which expressed AM, CLR and RAMP3 mRNA) to ascertain their effects on cancer cell viability and apoptosis *in vitro*. Lead compounds **7** and **8** were both able to decrease pancreatic cancer cell viability by up to 40% and 31% respectively, after 9 days of daily treatment at 3 µM concentration (Figure 3a, $p<0.05$). To control for CGRP receptor-mediated effects, we treated cultures of CFPAC-1 cells with rimegepant, a highly selective CGRP antagonist (pIC_{50} = <5 for AM_2 and 9.90 for CGRP receptors, Figure S4) and saw no significant reductions in viability (Figure 3a). **7** and **8** were also able to enhance levels of apoptosis markers (Caspases 3 and 7) in serum-starved pancreatic cancer cells by up to 50% and 104% respectively, 24 hours after treatment with varying concentrations between 3 µM and 100 nM (Figure 3b, $p<0.05$).

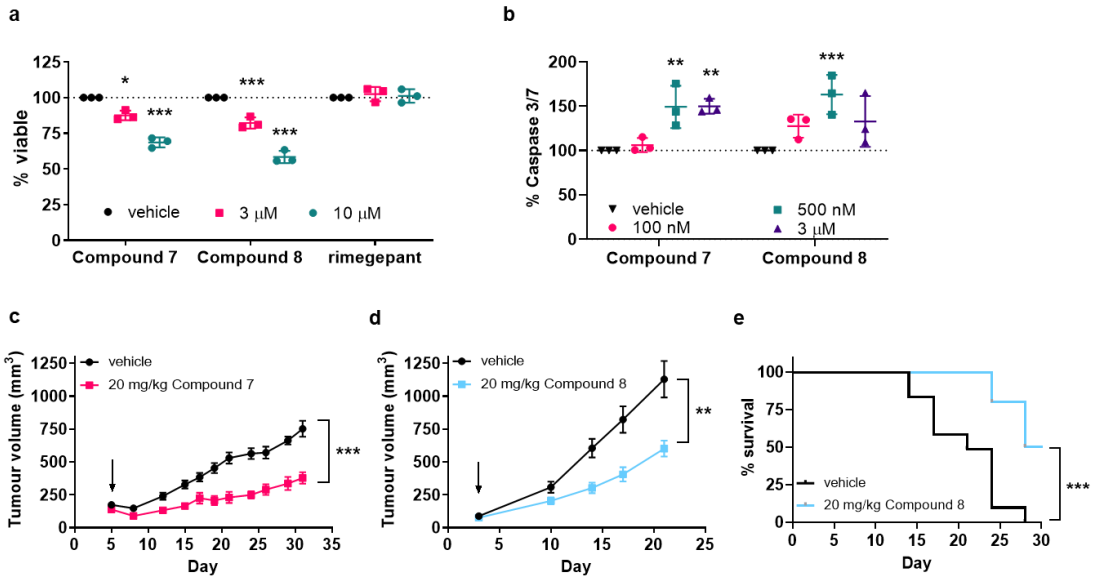

Figure 3: Effect of AM_2 receptor antagonists on *in vitro* viability and apoptosis of human pancreatic cancer cell line CFPAC-1 as well as subcutaneous CFPAC-1 tumor growth and survival in Balb/c nude mice. (**a**) Daily treatment with small molecule AM_2 receptor antagonists significantly decreased viability of CFPAC-1 in a concentration-dependent manner ($p<0.001$). Viability was decreased by up to 42% after 6 days when treated with either antagonist, compared to vehicle-treated controls ($p<0.001$). **8** had significantly greater effect in decreasing viability of CFPAC-1, compared to **7** ($p<0.001$). Rimegepant did not affect CFPAC-1 viability at tested concentrations (3 and 10 μM). Data are from three independent experiments and presented as mean±SD. (**b**) Treatment with various concentrations of small molecule AM_2 receptor antagonists significantly increased apoptosis of serum-starved (stressed) CFPAC-1 by up to 63% after 24 hours, compared to vehicle-treated stressed controls ($p<0.001$). Data are from three independent experiments and presented as mean±SD. (**c**, **d**, **e**) Mice were inoculated with CFPAC-1 tumors and first treatment was given on the day of first tumor volume measurement (arrows). Tumor growth rates were significantly reduced in mice treated daily with **7** (**c**, $p<0.001$) or **8** (**d**, $p<0.01$). n=6-7 (**c**) or n=10 (**d**) mice per group (**e**) Kaplan-Meier survival curves showed daily treatment with 20 mg/kg **8** significantly improved median survival to humane endpoint compared to vehicle-treated mice (29.5 vs. 21 days, $p<0.001$). Data presented as percentage of population. n=10 mice per group. *$p<0.05$, ** $p<0.01$, *** $p<0.001$

In order to gain insights into the potential therapeutic index of these AM_2 receptor antagonists, *in vivo* efficacy studies were conducted. **7** and **8** (20 mg/kg) or a vehicle control were administrated i.p. once daily, following the inoculation of tumor cells subcutaneously under the skin of the flank of Balb/c nude mice. Tumors were measured twice weekly to monitor the tumor growth and the well-being of the mice was assessed by measuring body weight and assessing appearance and behaviour. Both compounds were well tolerated and body weight increases were not significantly different in treatment and vehicle control groups. No adverse effects were observed from administration, and all mice behaved normally during the experiments, exhibiting apparently normal activity, feeding and inquisitiveness.

Daily administration of **7** was associated with significant inhibition in pancreatic xenograft tumor growth of 56% at week 5 ($p<0.001$, Figure 3c). Similar results were observed upon administration of **8** (20 mg/kg) where after three weeks of treatment, there was significantly reduced growth of tumors by 44% in the **8**-treated group ($p<0.01$, Figure 3d). While the experiments were not permitted to continue until the death of the animals from the tumors, we used as a surrogate for lifespan, the time taken for tumors to reach the local welfare regulatory authority (UK Home Office) maximum permitted size, at which the animals were euthanized. By this measure, mice treated with 20 mg/kg **8** have increased surrogate survival rates compared with vehicle-treated mice ($p<0.001$, Figure 3e) where at 28 days, all the vehicle treated mice had been euthanized but half the **8**-treated group were still alive.

AM_2 receptor antagonist inhibits proliferation, cancer-associated fibroblast expression and blood vasculature in pancreatic tumors *in vivo* in mice

To determine the mechanisms for the observed *in vivo* tumor growth inhibition as a result of AM_2 antagonist treatment, histological analysis was performed on subcutaneous human CFPAC-1 tumors from *in vivo* mice studies. Daily administration of **7** (20 mg/kg) was associated with significant decrease in markers of proliferation (Ki67, $p<0.01$, Figure 4a), cancer-associated

fibroblasts (alpha smooth muscle actin, αSMA, p<0.01, Figure 4b) and blood vasculature (CD31, p<0.05, Figure 4c), compared to vehicle-treated tumors.

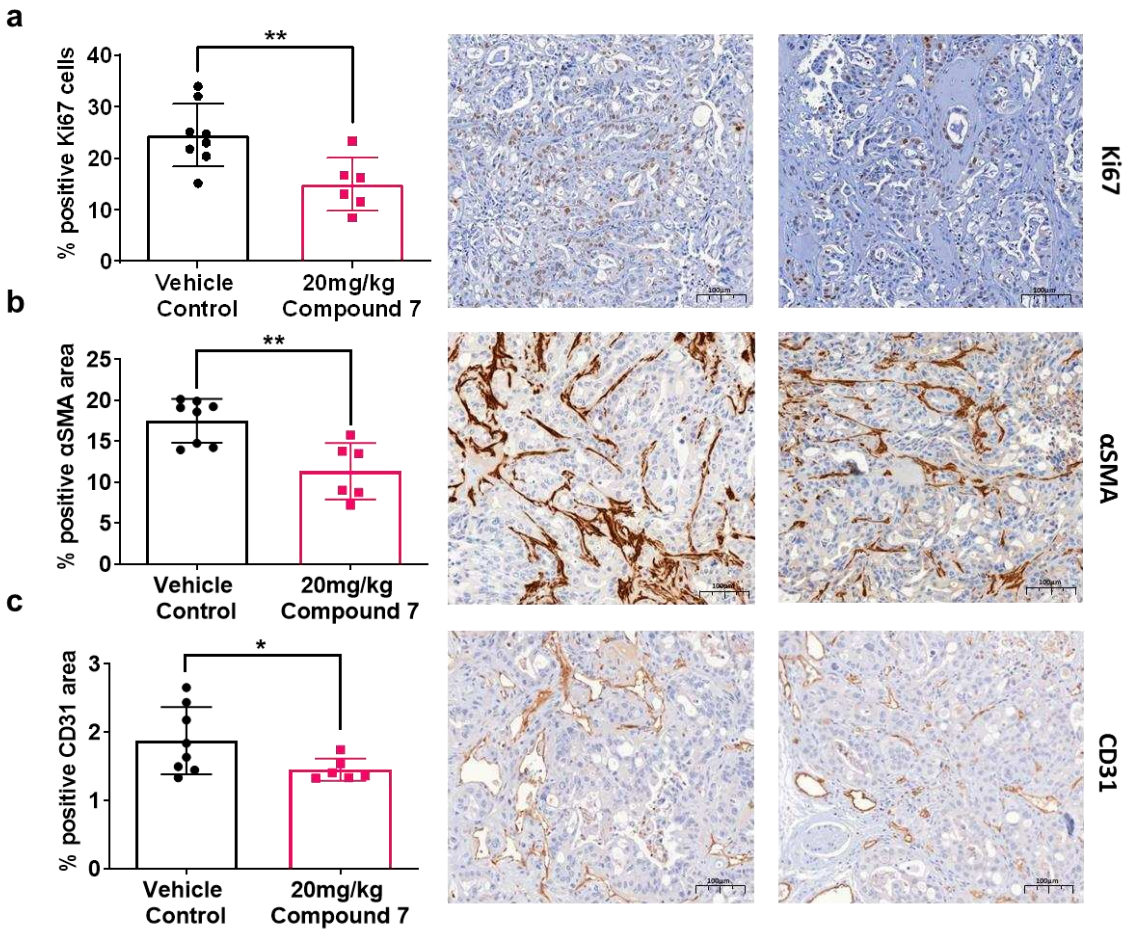

Figure 4. Histological analysis of AM_2 receptor antagonist treatment on *in vivo* subcutaneous CFPAC-1 tumor growth in Balb/c nude mice. (a-c) Daily treatment with compound **7** (20 mg/kg) significantly inhibited markers of proliferation (Ki67, p<0.01), cancer-associated fibroblasts (αSMA, p<0.01) and blood vasculature (CD31, p<0.05) in CFPAC-1 subcutaneous tumors. Data are presented as mean±SD. Representative images of control and AM_2 receptor antagonist-treated tumor sections are shown to the right of graphical data. *p<0.05, ** p<0.01

Here, we show the development and characterization of new potent first-in-class AM_2 receptor antagonists. The compounds we describe have very good selectivity over the AM_1, amylin and calcitonin receptors. Our best compound to date (compound 7) shows also just under 10-fold selectivity over the CGRP receptor. These molecules will aid understanding and the ability to manipulate this heteromeric receptor system with molecular precision. Specifically, through our structure/knowledge-based drug modelling approach, with its basis on CGRP antagonists and their reported interactions with the CGRP receptor, we have been able to develop the first highly potent and selective AM_2 receptor antagonists. These agents will allow significant new insights into the pharmacology of receptors combining the CLR with the 3 RAMPs because until now, the CGRP antagonists and anti-CGRP antibodies, less than fully characterized RAMP antibodies and non-selective peptide antagonists were the only tools available for such research.

Our modelling was based upon the published crystal structures of the CLR/RAMP1 CGRP receptor and the CLR/RAMP2 AM_1 receptor, with and without docked compounds. For our studies, despite the lack of a crystal structure for the CLR/RAMP3 AM_2 receptor, we created a hybrid model combining crystal structure information from the CLR domains of the CGRP and AM_1 receptors with a predicted structure for the RAMP3 domain. The model has been optimized slightly during the course of our work, as a result of hypothesis-testing compound generation to strengthen knowledge over uncertainties around specific domains. However, the model has proved to be of significant value in our design strategy and has allowed us to deliver the molecules that we report here. With the recent publication of cryo-EM structures of the full RAMP/receptor complexes novel sites for antagonism may be identified [34, 35].

Chemical synthesis of our compounds has not been completely straightforward, but during the course of our studies, problems have been solved to provide a robust high-yielding synthetic route. The route currently has 18 steps from inexpensive commercially available materials and is scalable to produce kilogram quantities of pure material.

The biological screening assay we have used is based upon inhibition of AM-induced cAMP synthesis in an engineered cell expressing the target receptor (AM_2 receptor for the first screen, and other receptors in response to their specific ligands for selectivity determinations). The major actions of AM are mediated predominantly via cAMP, so that it is unlikely we have missed compounds with effects mediated by other signalling mechanisms [51].

Functional studies of our compounds show consistent effects in a range of cancer model systems and across species (human, mouse and dog). Native cancer cells exhibit the same pharmacology as our engineered screening cells, with almost identical pIC_{50} values and the same preferential sensitivity to the stereoisomer **8** over **9**. Differences in pharmacology were shown across the species used with both compounds **7** and **8** showing lower efficacy on mouse and dog cells compared with human. However, it is unclear whether the observed pharmacological differences are due to differences between species or receptor expression. The *in vitro* cancer cell models comprise ways to measure cell viability and apoptosis (programmed cell death), both accepted *in vitro* markers of anti-tumor cell activity. The ADME and PK properties of **8** and **7** were found to suitable for *in vivo* studies in mice, such that i.p. administration at approximately 10mg/kg provided unbound plasma concentrations several fold higher than their in vitro AM_2 IC_{50} values. The effects of **8** (and the racemic mixture **7**) *in vivo* are clear, and are associated with what would be valuable likely increases in lifespan if replicated in human clinical patients. As these compounds have only ~10-fold selectivity over CGRP receptors, it was important to determine whether the effects we saw were due to antagonism of AM_2 or CGRP receptors. Use of the highly selective CGRP antagonist rimegepant (pIC_{50} = <5 for AM_2 and 9.90 for CGRP receptors), which is effectively incapable of blocking AM_2 receptors, revealed no inhibition of pancreatic tumor cell viability. Further clarification of this could be achieved by *in vitro* and *in vivo* xenograft studies using cells lacking either CGRP or AM2 receptors and treated with AM2 antagonists

One feature of our studies could suggest that effects of AM_2 antagonists in our mouse xenograft studies under-estimate benefits in humans. Our compounds are designed to block the human

AM_2 receptor and in the animal models they act on intrinsic signalling in the human tumor cells of the xenografts. However, tumor-secreted AM also acts on host cells in the tumor microenvironment as key RAMP residues in peptide-binding sites are conserved across many species including mouse[30]. On mouse cells (responding to AM expressed by the human tumor cells), our compounds are 2- to 100-fold less potent than on human cells. CGRP antagonists have historically shown even lower affinity in other species (including rodent and canine) compared to primates [52, 53]. If tumor-host interactions mediated by AM are an important feature of some clinical patient groups, then our compounds could provide more potent inhibitory effects than seen in mice by the increased potency on the human host AM_2 receptors. The lack of detectable side-effects in our studies are consistent with data showing that RAMP3 knockout mice (which are unable to make AM_2 receptors) are viable and healthy [19], and that in humans, an inactivating single nucleotide polymorphism in the gene for RAMP3 is represented in populations of healthy women [28].

In vitro effect of AM_2 receptor antagonists on cancer cell viability and apoptosis are significant but modest, compared to their potency in cAMP inhibition and the effect on *in vivo* tumor growth. The data suggest that AM may not be the main driver of cancer cell proliferation or apoptosis evasion, but instead, the creation of a pro-tumoral microenvironment. Models used in drug discovery for oncology all have limitations and provide somewhat simplistic answers to the major question of whether a candidate molecule could work in human clinical disease.

Histological analysis of tumor tissues revealed that anti-tumor effect of AM_2 receptor antagonists are not confined to tumor cells, but also stromal components of the tumor microenvironment including cancer-associated fibroblasts and blood vasculature originating from host non-tumor cells. This is an important property as 90% of pancreatic tumor mass is composed of fibrous desmoplastic stroma which impedes delivery of therapeutic agents to pancreatic cancer cells within the dense tumor [54]. Dai and colleagues have shown using *in vivo* gene knockout techniques that inhibition of AM-RAMP3 system and activation of AM-RAMP2 system suppressed

pancreatic tumor metastasis resulting from recruitment of cancer-associated fibroblasts [45]. Additionally, AM has also been shown to mediate desmoplasia in pancreatic cancer by mediating the effect of MYB on pancreatic cancer cells and cancer-associated fibroblasts both *in vitro* and *in vivo* [55].

Taken together, our data exemplify the strength of a rational drug design process to develop specific new antagonist molecules when sufficient structural information exists on targets, and there is access to a strong focused chemical starting point. We anticipate that our lead compounds will be the basis for improved molecules that will prove suitable in increasing understanding of fundamentals of the endocrinology of heteromeric receptors and as drug candidates for clinical development in pancreatic cancer.

Materials and Methods

All reagents, unless otherwise stated, were obtained from commercial sources and used without further purification. Olcegepant, telcagepant, rimegepant and MK-3207 were purchased from MedChemExpress (MCE) and were reconfirmed for its activity. Details are available in Supporting information. Small molecule antagonists were prepared as 2 mM DMSO stocks for cell culture experiments and stored at -20°C. Based on each cell lines ligand-receptor combination the appropriate unlabelled peptide was used. Human CGRP was obtained from Sigma Aldrich (SCP0060), rat AMY (rAMY) and human calcitonin (hCTR) were purchased from Bachem (H-9475 and H-2250 respectively) and human AM was purchased from Anaspec (AS-60447).

Compound synthesis and characterization

Compounds synthesis and characterization data are included in Supporting Information page S6.

Modelling and docking

Modelling and docking information are included in Supporting Information page S27

Cell lines and culture conditions

All cell lines were purchased from ATCC, Cell Applications, Inc or DiscoverX with proof of authentication, unless stated. All cell lines were maintained at 37°C in a humidified atmosphere with 5% CO_2. Human pancreatic cancer cells CFPAC-1 (ATCC, CRL-1918) were cultured in Dulbecco's Modified Eagle Medium (DMEM, Thermo Fisher Scientific, 61965-026) containing 10% (v/v) fetal bovine serum (FBS, Thermo Fisher Scientific, 10500-064) and 1% (v/v) penicillin–streptomycin (Sigma Aldrich, P4333). Canine aortic endothelia (CnAOEC) cells (Cell Applications, Cn304-05) were cultured in Canine EC Growth Medium Kit (Cell Applications, Cn211K-500). Mouse prostate cancer cells 178-2 BMA was obtained from Dr Timothy C. Thompson from the University of Texas MD Anderson Cancer Centre[56]. These cells were cultured in Dulbecco's Modified Eagle Medium (DMEM, Thermo Fisher Scientific, 61965-026) containing 10% (v/v) fetal bovine serum (FBS, Thermo Fisher Scientific, 10500-064), 1% HEPES and 1% (v/v) penicillin–

streptomycin (Sigma Aldrich, P4333). CGRP receptor, AM_1 receptor, AM_2 receptor, AMY_1 receptor, AMY_3 receptor and CTR overexpressing cell lines were obtained from DiscoverX (catalogue numbers, culture and selection information in Table S5). The RAMP/receptor component expression of these cells were validated in-house (Table S7).

Time-resolved fluorescence resonance energy transfer (TR-FRET) cAMP accumulation

The functional properties of compounds in GPCR/RAMP overexpressing cells (i.e. AM_2, CGRP, AM_1, AMY_1 and AMY_3 cells) as well as in human pancreatic cancer cells (CFPAC-1), in canine aortic endothelia (CnAOEC) cells and in mouse prostate cancer cells (178-2 BMA) were evaluated for their ability to inhibit cAMP production induced by an EC_{50} concentration of the maximum agonist activation (concentrations for each overexpressing cell line can be found in figure S5, table S6 and table S8 for the naïve cells). . Each compound was tested at 8 full-log concentrations (10^{-11} to 10^{-5} M) including a negative control (blank). The total cAMP was measured using the TR-FRET LANCE cAMP detection kit (PerkinElmer, AD0264), according to the manufacturer's directions. Aliquots of frozen cells (2×10^6 each) were thawed and prepared in warm stimulation buffer (1 × HBSS, 5 mM HEPES, 0.5 mM IBMX, and 0.1% BSA). Alexa Fluor antibody (1:100 concentration) was then added to the cell suspension and cells were plated (2,500 cells, 6 µL) in a 384-well white opaque microtiter plate (OptiPlates, Perkin Elmer, 6007299). Cells were first pre-incubated with serial dilutions (3 µL) of the antagonists for 30 minutes at room temperature prior to their stimulation with the EC_{50} value of agonist (3 µL) for 15 minutes at room temperature. Subsequently, 12 µL detection mix (Europium-Chelate streptavidin/biotinylated cAMP) was added to stop the reaction and induce cell lysis. TR-FRET was detected after an hour incubation by an EnSight multimode Plate reader (Perkin Elmer), at; 320/340 nm excitation and 615/665nm emission. Data were normalized to agonist only and blank (stimulation buffer only) wells as 0% and 100% cAMP inhibition, respectively.

The final DMSO concentration was below 0.5% and this was kept consistent in all the wells, including agonist alone and blank. The same methodology (including the number of cells) was

used for all cell lines. Concentration-response curves were analysed using three-parameter logistic curve to determine IC_{50} values (Graphpad Prism 7 and 8). No further constrains in any parameters of the curves were used.

In vitro viability and apoptosis assays

RealTime-Glo MT Viability Assay

Cell viability in human pancreatic cancer cells (CFPAC-1) was quantified using RealTime-Glo MT Cell Viability Assay (Promega, G9712). Cells (2,000 cells) were seeded into 96-well white clear-bottom plates (Corning, 3903) in full serum media overnight before washing and changing to sub-optimal media (DMEM + 5% FBS + 1% P/S) containing RealTime-Glo™ reagents according to Promega protocol. A baseline luminescence read (prior to treatment) was taken using EnSight Multimode Plate Reader (PerkinElmer) after an hour of incubation at 37°C. Cells were then treated with compounds or vehicle-control (PBS + 0.05% DMSO) daily. Results were normalized to vehicle-treated controls as 100% viable (Graphpad Prism 7 and 8).

Caspase-Glo 3/7 Apoptosis Assay

The effect of the compounds on cell apoptosis in human pancreatic cancer cells (CFPAC-1), was determined using luminescence-based Caspase-Glo™ 3/7 Assay (Promega, G8093). This end-point assay measures late-stage apoptotic markers – caspases 3 and 7. Cells (20,000 cells) were seeded into 96-well white clear-bottom plates (Corning, 3903) Cells were then treated for 24 hours with compounds (or vehicle-control) diluted in PBS (0.05% DMSO). Caspase-Glo™ reagent was prepared according to Promega protocol and added to the cells. Each sample was incubate for 30 to 60 minutes on a plate shaker (550 rpm). Luminescence read was then taken using EnSight Multimode Plate Reader (PerkinElmer) set to 22°C. Baseline readings (media only) were subtracted from sample luminescence readings. Results were normalized to unstressed controls (optimal growth media) and serum-starved vehicle controls as 0% and 100% apoptosis, respectively (Graphpad Prism 7 and 8).

ADME and physicochemical assays

Kinetic solubility

Compounds initially dissolved at a concentration of 10 mM in DMSO were diluted in 50 mM phosphate buffer (pH 2 or 7.4) to a concentration of 200 µM, followed by vigorous shaking for 24 h at room temperature. Precipitated material was then removed by filtration and the remaining compound concentration was established using UV absorbance.

Microsomal stability assays

Metabolic stability of compounds was assessed in the presence of human (Corning, 452117), rat (Xenotech, R1000) or mouse (Xenotech,M1000) microsome suspensions in 100 mM potassium phosphate buffer at a protein concentration of 0.5 mg/ml. 10 µL of a solution of 10 µM of each test compound or positive controls (testosterone, diclofenac and propafenone) were added into the appropriate wells of 96-well plates (a matrix blank was also included). 80 µL of microsomal suspension was added to test compound followed by incubation for 10 min at 37°C. Reactions were initiated by addition of 10 µL of pre-warmed NADPH (β-Nicotinamide adenine dinucleotide phosphate) and plates were incubated at 37ºC. Reactions were stopped after 60, 30, 20, 10, 5 and 0 min by the addition of 300 µL/well of cold (4ºC) stop solution (100 ng/mL tolbutamide and 100 ng/mL labetalol). Sample plates were then shaken for 10 minutes followed by centrifugation at 4000 rpm for 20 min at 4ºC. Rates of decrease in compound over time were determined using LC-MS/MS and microsomal intrinsic clearance (CL_{int}) was then calculated.

Plasma stability assays

A known concentration of compound (0.1-1 µM) was incubated in the presence of human (BioIVT, HMPLEDTA2), rat (BioIVT, RATPLEDTA2-M) or mouse (BioIVT, MSE00PLK2M2N) plasma (80% in PBS, pH 7.4) for up to 120 min (0, 5, 15, 30, 60, 120 min). Propantheline bromide was used as reference compound. At the end of each time point the % of the remaining compound concentration compared to time point 0 was determined using LC-MS/MS.

Plasma Protein Binding (PPB) assays

PPB was determined using an equilibrium dialysis assay in which a semi-permeable membrane separates two compartments, one of which contains undiluted plasma containing added test compound (2 µM) and the other containing buffer (Dialysis Buffer -100 mM sodium phosphate and 150 mM NaCl, pH 7.4 ± 0.1). The system is then incubated at 37°C until equilibrium was reached (5% CO_2 at 37±1˚C for 4 hours and the amount of test compound in each compartment was then analysed using LC-MS/MS. The fraction of unbound compound)Fu(was then calculated using the relationship Fu = concentration in buffer/ concentration in plasma. Known control compounds, including verapamil and warfarin, were used for assay validation.

Cytochrome P450 (CYP450) enzymes inhibition assays

Five different cytochrome P450 isoforms (1A2, 2C9, 2C19, 2D6 and 3A4) were investigated with cytochrome P450 enzyme inhibition assays. Specific substrates (Table S9) for each isoform were incubated with a range of test compound concentrations (0-50µM) in the presence of human liver microsomes. At the end of the incubation, the formation of a known metabolite depending on the isoform was monitored using LC-MS/MS. The ability (IC_{50}) of each test compound to inhibit the formation of the metabolites was then measured compared to the vehicle control. Known positive inhibitors of each isoform were also used for assay validation (Table S9).

hERG channel test

To evaluate the effects of test compounds on the hERG potassium channels, the automated patch clamp method ($QPatch^{HTX}$) was used. CHO cells stably expressing hERG potassium channels (Aviva Biosciences) were used for this test at 75% confluency or more. Before testing, cells were harvested using TrypLE and resuspended in the extracellular solution at the room temperature. All solutions used for the electrophysiological recordings are shown in Table S10.

Test compounds and positive control (Amitriptyline) were dissolved in 100% DMSO to obtain stock solutions for different test concentrations. Then the stock solutions were further diluted into

extracellular solution to achieve final concentrations for testing (final DMSO concentration not more than 0.3%).

Voltage command protocol: From the holding potential of -80 mV, the voltage was first stepped to -50 mV for 80 ms for leak subtraction, and then stepped to +20 mV for 4800 ms to open hERG channels. After that, the voltage was stepped back down to -50 mV for 5000 ms, causing a "rebound" or tail current, which was measured and collected for data analysis. Finally, the voltage was stepped back to the holding potential (-80 mV, 3100 ms). This voltage command protocol was repeated every 15000 msec. This command protocol was performed continuously during the test (vehicle control and test compound).

QPatch^{HTX} Whole-cell recording: hERG QPatch^{HTX} assay was conducted at room temperature. All protocols were established and performed using QPatch Assay Software 5.6 (Sophion Bioscience). Three additions of 5 µl of the vehicle were applied, followed by 30 runs of voltage protocol for a baseline period. Then the ascending concentrations of each compound were added with three repetitions (5 µl*3). The exposure of test compound at each concentration was no less than 5 minutes. Five concentrations (0.37 µM, 1.11 µM, 3.33 µM, 10 µM and 30 µM) were tested for each compound (minimum 2 replicates per concentration).

Within each well recording, percent of control values were calculated for each test compound concentration current response based on peak current in presence of vehicle control. Curve-fitting and IC50 calculations were performed by QPatch Assay Software. If the inhibition obtained at the lowest concentration tested was over 50%, or at the highest concentration tested was less than 50%, we reported the IC50 as less than lowest concentration, or higher than highest concentration, respectively.

Ethical statement for *in vivo* studies

All *in vivo* experiments were performed according to the regulations of the UK Animals (Scientific Procedures) Act 1986 (ASPA) and after the approval of Home Office and local research ethics

committees through the granting of project and personal licenses for the studies. Where studies were performed outside of the UK and not directly under those mandatory legal constraints, methodology and conditions were approved before the studies by the National Council for the 3Rs (Reduction, Refinement and Replacement) and the Wellcome Trust.

Pharmacokinetic (PK) studies

PK studies were performed in mice and rats using i.v., p.o. and i.p. routes of administration. Each mouse study was performed using 3 male (7-9 weeks old) CD-1 mice (source: WTLH Laboratory Animal Co. Ltd. or SIPPR-B&K Laboratory Animal Co. Ltd.). Rat PK studies were performed using 3 male (7-9 weeks old) Sprague Dawley (SD) rats (source: SLAC Laboratory Animal Co. Ltd. or WTLH Laboratory Animal Co. Ltd.). Compounds were accurately weighed and dissolved in the appropriate volume of vehicle (50% PEG E 400/50% water or 10% DMSO/50% Solutol/40% water). The solution was sonicated in a water bath until clear solution (i.v and i.p dosing) and uniform suspension (p.o dosing) was obtained, pH adjusted if needed and sterile filtered prior to administration. For i.v dosing, the compounds were administered via tail vein following the facility's SOPs. For oral dosing (p.o) compounds were administered by oral gavage. For i.p dosing the compounds were injected in the animal's lower right quadrant of the abdomen following the facility's SOPs. The dose volume was determined by the animals' body weight collected on the morning of dosing day.

At different time points after administration, approximately 0.25 mL (in rats) and 30µL (in mice) of blood was collected from each animal (via jugular vein or another suitable vein - in rats via the saphenous vein or in mice, the submandbular vein). At each time point, the animals were restrained and the blood sample was taken using a needle and while observing aseptic precautions. Samples were transferred into ice cold microcentrifuge tubes containing 5 µL of anti-coagulant (0.5 M EDTA-K_2). Samples were then centrifuged at 3,000 g at 4^{o}C for 15 min. Plasma samples were then collected and stored in polypropylene tubes at -80^{o}C until quantification by

LC-MS/MS analysis. Upon completion of the studies animals were euthanised using Carbon dioxide (CO_2) overdose (Carbon Dioxide Euthanasia).

In vivo efficacy models

In these studies, we used 6-7 week old BALB/c nude female mice, with a weight range of 15-20g. Animals were provided by Envigo Corporation (Cambridgeshire, UK) or Charles River Laboratories (Massachusetts, USA) depending on availability. Each experiment started with 10 mice (experimental units) in each experimental/control group. Subsequent analysis (tumor growth and histology) was only performed in animals where tumors had established and were palpable within 3 days of implantation. This was in accordance with power calculation performed to ensure robust statistical analysis by The University of Sheffield Statistical Service. Implanting cells into 10 animals in each group ensured that we had a minimum of 6 mice completing the procedure in all our studies. Where tumors established in more than 6 mice, all were included for data analysis. The animals were housed in individually ventilated cages (IVCs) (with the appropriate bedding and flooring conditions) in environmentally controlled conditions with a 12 hr light/dark cycles at ~26°C. Mice had access to adequate amount of water and 2018 Teklad Global 18% Protein Rodent Diet containing 1.01% Calcium (Harlan Laboratories, UK). The day-to-day care of the animals was carried out by the technicians in the Biological Services (The University of Sheffield, UK). All scientific procedures on animals were carried under UK Home Office Project Licenses (40/3499 or PF61050A3) and Procedure Individual Licenses.

Compound preparation for *in vivo* studies

Compounds were dissolved in DMSO (Sigma Aldrich, D4540) and sonicated at 37°C for 10 mins. Appropriate volume of solvent (Kolliphor HS15 (1 part, grams), Kollisolv PEG E 400 (3 parts, mL) and PBS (6 parts, mL)) was then added to yield a 6% DMSO/94% solvent solution. These working stocks (8 mg/mL) were further sonicated at 37°C for 10 mins before storing at -20ºC. To make treatment aliquots, equal amounts of the working stock (or vehicle-control) and solvent were mixed and sonicated at 37°C for 10 mins (4 mg/mL, equivalent to 20 mg/kg, 3% DMSO/97%

solvent). Vehicle-control and compounds were sonicated at 37°C for 10 mins prior to i.p. injections (200 µL per mouse).

Cell preparation and tumor inoculation

Cells were prepared according to standard cell culture techniques. Cell pellets were resuspended in 50% PBS/50% Matrigel (Corning, 354234). Matrigel/PBS cell suspension, needles (25G) and syringes (1 mL) were kept on ice before and during tumor inoculation into mice. Cell suspension (100 µL, 5 × 106 cells) was injected subcutaneously into the left flank of 6-7 weeks old female immunodeficient nude athymic mice (Balb/c nude). Once the tumors became palpable (around 100 mm^3), mice were randomized into treatment groups. Mice were treated daily by i.p. injection at the same time of day with 20 mg/kg of compound or vehicle-control (200 µL per mouse) until humane end-point. Mice were observed for at least 30 mins post-treatment to detect any acute adverse effects. Tumor size and mouse weights were measured twice a week. At the end of each study the animals were euthanized following the appropriate procedures listed in ASPA Act 1986. Vital organs and tumors were stored in 10% neutral-buffered formalin for further histological analysis. Primary experimental outcome was tumor volume with additional measurement of molecular markers in tissue and serum as well as time to humane endpoint. Blinding was not used for the *in vivo* studies.

Immunohistochemistry (IHC)

Immunohistochemical detection of CD31 (Dianova, DIA-310), Ki67 (Abcam, ab15580) and αSMA (Abcam, ab124964) was performed in paraffin-embedded tumor sections obtained from the *in vivo* studies using ABC system (Vector Laboratories). All stained slides were scanned using Panoramic 250 Flash III slide scanner (3DHISTECH). Specific protocols used can be found in Table S11. Sections were dewaxed in a graded xylene/ethanol series and antigens were retrieved by incubating the slides in Tris-EDTA (TE) buffer (Fisher Scientific) for 20 minutes using a conventional food steamer (for Ki67) or by incubating the slides in a 95°C PT module (Thermo Scientific) containing 1x citrate buffer (pH 6) (Abcam) for 25 minutes (for CD31 and αSMA).

Endogenous peroxidase was then blocked by incubating slides in 3%H_2O_2 (Sigma-Aldrich) in distilled H_2O for 30 minutes at RT. Slides were then blocked with 1.5% blocking serum (ABC VECTASTAIN IgG Kit) and incubated with the primary antibody (concentrations can be found in Table S11) at 4°C overnight (1 hour at RT for Ki67). After successive incubations (30 minutes at RT) with the corresponding biotinylated IgG (Vector Laboratories) and the ABC solution (Vector Laboratories), the peroxidase activity was developed using 3, 3'-Diaminobenzidine (DAB) (ImmPACT™ DAB EqV) as a substrate. Slides were counterstained with Gill's hematoxylin (Merck) for 20 seconds, dehydrated, and mounted with coverslips using DPX (distyrene, plasticizer and xylene mixture) mounting medium (Sigma-Aldrich).

Immunohistochemistry (IHC) analysis

QuPath v0.1.2, an open source digital pathology software was used to identify and count the positive cells (brown) in Ki67 stained sections. The whole tumor sections were selected as regions of interest (ROIs) and the positive cell detection command was performed, using the single threshold option, to distinguish and quantify the brown stained (positive) cells from the negative hematoxylin (blue) stained cells. For the αSMA stained sections ImageJ v1.49 was used for analysis. The whole tumor sections were selected as regions of interest (ROIs). Using the colour threshold tool, brown DAB (positive) staining was highlighted while all blue hematoxylin (negative) stained sections were excluded. Masks of the highlighted regions were then generated and were used to measure the percentage area of positive staining. Similarly, the same procedure was used for the analysis of CD31 sections however, only four snapshots (ROIs) per slide were used due to the low intensity of the CD31 staining.

Statistics

For cAMP accumulation studies all data consist of at least three independent experimental repeats. Each independent experimental repeat is performed on a new batch of cells and on a separate date from the previous repeat. Curves shown are representative and do not include all data points. Data points and curves are presented as mean±SEM and significance were defined

by unpaired t-test. Student's t-test or one-way ANOVA were used to compare between groups of one experimental variable. In experiments where there are more than one experimental variable, two-way ANOVA was used to analyse individual variables and the interaction between them. Repeated-measures two-way ANOVA was used to analyse time course data and normalised data (e.g. viability and apoptosis data). Post-hoc multiple comparisons tests (Dunnett or Tukey) were also used to determine statistical significance of differences. Log-rank test was used to compare Kaplan-Meier survival curves.

Data availability

All data generated or analysed during this study are either included in this published article (and its supplementary information) or are available from the corresponding authors on reasonable request.

References

1. Yallampalli, C., Chauhan, M., Sathishkumar, K., Calcitonin Gene-Related Family Peptides in Vascular Adaptations, Uteroplacental Circulation, and Fetal Growth. *Current Vascular Pharmacology* **2013,** *11* (5), 641-654.
2. Sandner, P., Hofbauer, K. H., Tinel, H., Kurtz, A., Thiesson, H. C., Ottosen, P. D., Walter, S., Skott, O., Jensen, B. L., Expression of adrenomedullin in hypoxic and ischemic rat kidneys and human kidneys with arterial stenosis. *American Journal of Physiology-Regulatory Integrative and Comparative Physiology* **2004,** *286* (5), R942-R951.
3. Hirata, Y., Mitaka, C., Sato, K., Nagura, T., Tsunoda, Y., Amaha, K., Marumo, F., Increased circulating adrenomedullin, a novel vasodilatory peptide, in sepsis. *Journal of Clinical Endocrinology & Metabolism* **1996,** *81* (4), 1449-1453.
4. Guignant, C., Voirin, N., Venet, F., Poitevin, F., Malcus, C., Bohe, J., Lepape, A., Monneret, G., Assessment of pro-vasopressin and pro-adrenomedullin as predictors of 28-day mortality in septic shock patients. *Intensive Care Medicine* **2009,** *35* (11), 1859-1867.
5. Marino, R., Struck, J., Maisel, A. S., Magrini, L., Bergmann, A., Di Somma, S., Plasma adrenomedullin is associated with short-term mortality and vasopressor requirement in patients admitted with sepsis. *Critical Care* **2014,** *18* (1).
6. Hay, D. L., Walker, C. S., Poyner, D. R., Adrenomedullin and calcitonin gene-related peptide receptors in endocrine-related cancers: opportunities and challenges. *Endocrine-Related Cancer* **2011,** *18* (1), C1-C14.
7. Aggarwal, G., Ramachandran, V., Javeed, N., Arumugam, T., Dutta, S., Klee, G. G., Klee, E. W., Smyrk, T. C., Bamlet, W., Han, J. J., Vittar, N. B. R., De Andrade, M., Mukhopadhyay, D., Petersen, G. M., Fernandez-Zapico, M. E., Logsdon, C. D., Chari, S. T., Adrenomedullin is Up-

regulated in Patients With Pancreatic Cancer and Causes Insulin Resistance in beta Cells and Mice. *Gastroenterology* **2012,** *143* (6), 1510-+.
8. Zudaire, E., Martinez, A., Cuttitta, F., Adrenomedullin and cancer. *Regulatory Peptides* **2003,** *112* (1-3), 175-183.
9. Martinez, A., Vos, M., Guedez, L., Kaur, G., Chen, Z., Garayoa, M., Pio, R., Moody, T., Stetler-Stevenson, W. G., Kleinman, H. K., Cuttitta, F., The effects of adrenomedullin overexpression in breast tumor cells. *Journal of the National Cancer Institute* **2002,** *94* (16), 1226-1237.
10. Weston, C., Winfield, I., Harris, M., Hodgson, R., Shah, A., Dowell, S. J., Mobarec, J. C., Woodlock, D. A., Reynolds, C. A., Poyner, D. R., Watkins, H. A., Ladds, G., Receptor Activity-modifying Protein-directed G Protein Signaling Specificity for the Calcitonin Gene-related Peptide Family of Receptors. *Journal of Biological Chemistry* **2016,** *291* (42), 21925-21944.
11. Hay, D. L., Pioszak, A. A., Receptor Activity-Modifying Proteins (RAMPs): New Insights and Roles. *Annual Review of Pharmacology and Toxicology* **2016,** *56* (1), null.
12. Barbash, S., Lorenzen, E., Persson, T., Huber, T., Sakmar, T. P., GPCRs globally coevolved with receptor activity-modifying proteins, RAMPs. *Proceedings of the National Academy of Sciences of the United States of America* **2017,** *114* (45), 12015-12020.
13. Mackie, D. I., Nielsen, N. R., Harris, M., Singh, S., Davis, R. B., Dy, D., Ladds, G., Caron, K. M., RAMP3 determines rapid recycling of atypical chemokine receptor-3 for guided angiogenesis. *Proceedings of the National Academy of Sciences of the United States of America* **2019,** *116* (48), 24093-24099.
14. McLatchie, L. M., Fraser, N. J., Main, M. J., Wise, A., Brown, J., Thompson, N., Solari, R., Lee, M. G., Foord, S. M., RAMPs regulate the transport and ligand specificity of the calcitonin-receptor-like receptor. *Nature* **1998,** *393* (6683), 333-339.
15. Edvinsson, L., Haanes, K. A., Warfvinge, K., Krause, D. N., CGRP as the target of new migraine therapies - successful translation from bench to clinic. *Nature Reviews Neurology* **2018,** *14* (6), 338-350.
16. Hay, D. L., Garelja, M. L., Poyner, D. R., Walker, C. S., Update on the pharmacology of calcitonin/CGRP family of peptides: IUPHAR Review 25. *British Journal of Pharmacology* **2018,** *175* (1), 3-17.
17. Tepper, S. J., History and Review of anti-Calcitonin Gene-Related Peptide (CGRP) Therapies: From Translational Research to Treatment. *Headache* **2018,** *58*, 238-275.
18. Hay, D. L., Howitt, S. G., Conner, A. C., Schindler, M., Smith, D. M., Poyner, D. R., CL/RAMP2 and CL/RAMP3 produce pharmacologically distinct adrenomedullin receptors: a comparison of effects of adrenomedullin(22-52), CGRP(8-37) and BIBN4096BS. *British Journal of Pharmacology* **2003,** *140* (3), 477-486.
19. Dackor, R., Fritz-Six, K., Smithies, O., Caron, K., Receptor activity-modifying proteins 2 and 3 have distinct physiological functions from embryogenesis to old age. *Journal of Biological Chemistry* **2007,** *282* (25), 18094-18099.
20. Ishikawa, T., Chen, J., Wang, J., Okada, F., Sugiyama, T., Kobayashi, T., Shindo, M., Higashino, F., Katoh, H., Asaka, M., Kondo, T., Hosokawa, M., Kobayashi, M., Adrenomedullin antagonist suppresses in vivo growth of human pancreatic cancer cells in SCID mice by suppressing angiogenesis. *Oncogene* **2003,** *22* (8), 1238-42.
21. Keleg, S., Kayed, H., Jiang, X., Penzel, R., Giese, T., Büchler, M. W., Friess, H., Kleeff, J., Adrenomedullin is induced by hypoxia and enhances pancreatic cancer cell invasion. *Int J Cancer* **2007,** *121* (1), 21-32.

22. D'Angelo, F., Letizia, C., Antolino, L., La Rocca, M., Aurello, P., Ramacciato, G. Adrenomedullin in pancreatic carcinoma: A case-control study of 22 patients 2016.
23. Brekhman, V., Lugassie, J., Zaffryar-Eilot, S., Sabo, E., Kessler, O., Smith, V., Golding, H., Neufeld, G., Receptor activity modifying protein-3 mediates the protumorigenic activity of lysyl oxidase-like protein-2. *Faseb Journal* **2011,** *25* (1), 55-65.
24. Ramachandran, V., Arumugam, T., Hwang, R. F., Greenson, J. K., Simeone, D. M., Logsdon, C. D., Adrenomedullin is expressed in pancreatic cancer and stimulates cell proliferation and invasion in an autocrine manner via the adrenomedullin receptor, ADMR. *Cancer Research* **2007,** *67* (6), 2666-2675.
25. Caron, K. M., Smithies, O., Extreme hydrops fetalis and cardiovascular abnormalities in mice lacking a functional Adrenomedullin gene. *Proceedings of the National Academy of Sciences of the United States of America* **2001,** *98* (2), 615-619.
26. Dackor, R. T., Fritz-Six, K., Dunworth, W. P., Gibbons, C. L., Smithies, O., Caron, K. M., Hydrops fetalis, cardiovascular defects, and embryonic lethality in mice lacking the Calcitonin receptor-like receptor gene. *Molecular and Cellular Biology* **2006,** *26* (7), 2511-2518.
27. Shindo, T., Sakurai, T., Kamiyoshi, A., Ichikawa-Shindo, Y., Shimoyama, N., Iinuma, N., Arai, T., Miyagawa, S., Regulation of Adrenomedullin and its Family Peptide by RAMP System - Lessons from Genetically Engineered Mice. *Current Protein & Peptide Science* **2013,** *14* (5), 347-357.
28. Prakash, J., Herlin, M., Kumar, J., Garg, G., Akesson, K. E., Grabowski, P. S., Skerry, T. M., Richards, G. O., McGuigan, F. E. A., Analysis of RAMP3 gene polymorphism with body composition and bone density in young and elderly women. *Gene: X* **2019,** *2*, 100009.
29. Serafin, D. S., Harris, N. R., Nielsen, N. R., Mackie, D. I., Caron, K. M., Dawn of a New RAMPage. *Trends in Pharmacological Sciences* **2020,** *41* (4), 249-265.
30. Booe, J. M., Walker, C. S., Barwell, J., Kuteyi, G., Simms, J., Jamaluddin, M. A., Warner, M. L., Bill, R. M., Harris, P. W., Brimble, M. A., Poyner, D. R., Hay, D. L., Pioszak, A. A., Structural Basis for Receptor Activity-Modifying Protein-Dependent Selective Peptide Recognition by a G Protein-Coupled Receptor. *Molecular Cell* **2015,** *58* (6), 1040-1052.
31. ter Haar, E., Koth, C. M., Abdul-Manan, N., Swenson, L., Coll, J. T., Lippke, J. A., Lepre, C. A., Garcia-Guzman, M., Moore, J. M., Crystal Structure of the Ectodomain Complex of the CGRP Receptor, a Class-B GPCR, Reveals the Site of Drug Antagonism. *Structure* **2010,** *18* (9), 1083-1093.
32. Moore, E. L., Gingell, J. J., Kane, S. A., Hay, D. L., Salvatore, C. A., Mapping the CGRP receptor ligand binding domain: Tryptophan-84 of RAMP1 is critical for agonist and antagonist binding. *Biochemical and Biophysical Research Communications* **2010,** *394* (1), 141-145.
33. Watkins, H. A., Walker, C. S., Ly, K. N., Bailey, R. J., Barwell, J., Poyner, D. R., Hay, D. L., Receptor activity-modifying protein-dependent effects of mutations in the calcitonin receptor-like receptor: implications for adrenomedullin and calcitonin gene-related peptide pharmacology. *British Journal of Pharmacology* **2014,** *171* (3), 772-788.
34. Liang, Y.-L., Khoshouei, M., Deganutti, G., Glukhova, A., Koole, C., Peat, T. S., Radjainia, M., Plitzko, J. M., Baumeister, W., Miller, L. J., Hay, D. L., Christopoulos, A., Reynolds, C. A., Wootten, D., Sexton, P. M., Cryo-EM structure of the active, G(s)- protein complexed, human CGRP receptor. *Nature* **2018,** *561* (7724), 492-+.
35. Liang, Y.-L., Belousoff, M. J., Fletcher, M. M., Zhang, X., Khoshouei, M., Deganutti, G., Koole, C., Furness, S. G. B., Miller, L. J., Hay, D. L., Christopoulos, A., Reynolds, C. A., Danev, R., Wootten, D., Sexton, P. M., Structure and Dynamics of Adrenomedullin Receptors AM1 and AM2

Reveal Key Mechanisms in the Control of Receptor Phenotype by Receptor Activity-Modifying Proteins. *ACS pharmacology & translational science* **2020,** *3* (2), 263-284.
36. Garelja, M. L., Au, M., Brimble, M. A., Gingell, J. J., Hendrikse, E. R., Lovell, A., Prodan, N., Sexton, P. M., Siow, A., Walker, C. S., Watkins, H. A., Williams, G. M., Wootten, D., Yang, S. H., Harris, P. W. R., Hay, D. L., Molecular Mechanisms of Class B GPCR Activation: Insights from Adrenomedullin Receptors. *ACS pharmacology & translational science* **2020,** *3* (2), 246-262.
37. Bell, I. M., Calcitonin Gene-Related Peptide Receptor Antagonists: New Therapeutic Agents for Migraine. *Journal of Medicinal Chemistry* **2014,** *57* (19), 7838-7858.
38. Hewitt, D. J., Aurora, S. K., Dodick, D. W., Goadsby, P. J., Ge, Y. J., Bachman, R., Taraborelli, D., Fan, X., Assaid, C., Lines, C., Ho, T. W., Randomized controlled trial of the CGRP receptor antagonist MK-3207 in the acute treatment of migraine. *Cephalalgia* **2011,** *31* (6), 712-22.
39. Ho, T. W., Ho, A. P., Ge, Y. J., Assaid, C., Gottwald, R., MacGregor, E. A., Mannix, L. K., van Oosterhout, W. P., Koppenhaver, J., Lines, C., Ferrari, M. D., Michelson, D., Randomized controlled trial of the CGRP receptor antagonist telcagepant for prevention of headache in women with perimenstrual migraine. *Cephalalgia* **2016,** *36* (2), 148-61.
40. Ho, T. W., Connor, K. M., Zhang, Y., Pearlman, E., Koppenhaver, J., Fan, X., Lines, C., Edvinsson, L., Goadsby, P. J., Michelson, D., Randomized controlled trial of the CGRP receptor antagonist telcagepant for migraine prevention. *Neurology* **2014,** *83* (11), 958-66.
41. NCT03237845, Safety and Efficacy in Adult Subjects With Acute Migraines - Full Text View - ClinicalTrials.gov.
42. NCT02828020, Efficacy, Safety, and Tolerability Study of Oral Ubrogepant in the Acute Treatment of Migraine - Full Text View - ClinicalTrials.gov.
43. Archbold, J. K., Flanagan, J. U., Watkins, H. A., Gingell, J. J., Hay, D. L., Structural insights into RAMP modification of secretin family G protein-coupled receptors: implications for drug development. *Trends in Pharmacological Sciences* **2011,** *32* (10), 591-600.
44. Hendrikse, E. R., Liew, L. P., Bower, R. L., Bonnet, M., Jamaluddin, M. A., Prodan, N., Richards, K. D., Walker, C. S., Pairaudeau, G., Smith, D. M., Rujan, R.-M., Sudra, R., Reynolds, C. A., Booe, J. M., Pioszak, A. A., Flanagan, J. U., Hay, M. P., Hay, D. L., Identification of Small-Molecule Positive Modulators of Calcitonin-like Receptor-Based Receptors. *ACS Pharmacology & Translational Science* **2020**.
45. Dai, K., Tanaka, M., Kamiyoshi, A., Sakurai, T., Ichikawa-Shindo, Y., Kawate, H., Cui, N., Wei, Y., Tanaka, M., Kakihara, S., Matsui, S., Shindo, T., Deficiency of the adrenomedullin-RAMP3 system suppresses metastasis through the modification of cancer-associated fibroblasts. *Oncogene* **2019**.
46. Bell, I. M., Gallicchio, S. N., Wood, M. R., Quigley, A. G., Stump, C. A., Zartman, C. B., Fay, J. F., Li, C. C., Lynch, J. J., Moore, E. L., Mosser, S. D., Prueksaritanont, T., Regan, C. P., Roller, S., Salvatore, C. A., Kane, S. A., Vacca, J. P., Selnick, H. G., Discovery of MK-3207: A Highly Potent, Orally Bioavailable CGRP Receptor Antagonist. *Acs Medicinal Chemistry Letters* **2010,** *1* (1), 24-29.
47. Wood, M. R., Schirripa, K. M., Kim, J. J., Quigley, A. G., Stump, C. A., Bell, I. M., Bednar, R. A., Fay, J. F., Bruno, J. G., Moore, E. L., Mosser, S. D., Roller, S., Salvatore, C. A., Kane, S. A., Vacca, J. P., Selnick, H. G., Novel CGRP receptor antagonists through a design strategy of target simplification with addition of molecular flexibility. *Bioorganic & Medicinal Chemistry Letters* **2009,** *19* (19), 5787-5790.

48. Wilkinson, G. R., Shand, D. G., PHYSIOLOGICAL APPROACH TO HEPATIC DRUG CLEARANCE. *Clinical Pharmacology & Therapeutics* **1975,** *18* (4), 377-390.
49. Yang, J., Jamei, M., Yeo, K. R., Rostami-Hodjegan, A., Tucker, G. T., Misuse of the well-stirred model of hepatic drug clearance. *Drug Metabolism and Disposition* **2007,** *35* (3), 501-502.
50. Rampe, D., Brown, A. M., A history of the role of the hERG channel in cardiac risk assessment. *Journal of Pharmacological and Toxicological Methods* **2013,** *68* (1), 13-22.
51. Huang, W., Wang, L., Yuan, M., Ma, J. X., Hui, Y. N., Adrenomedullin affects two signal transduction pathways and the migration in retinal pigment epithelial cells. *Investigative Ophthalmology & Visual Science* **2004,** *45* (5), 1507-1513.
52. Doods, H., Hallermayer, G., Wu, D. M., Entzeroth, M., Rudolf, K., Engel, W., Eberlein, W., Pharmacological profile of BIBN4096BS, the first selective small molecule CGRP antagonist. *British Journal of Pharmacology* **2000,** *129* (3), 420-423.
53. Salvatore, C. A., Moore, E. L., Calamari, A., Cook, J. J., Michener, M. S., O'Malley, S., Miller, P. J., Sur, C., Williams, D. L., Zeng, Z. Z., Danziger, A., Lynch, J. J., Regan, C. P., Fay, J. F., Tang, Y. S., Li, C. C., Pudvah, N. T., White, R. B., Bell, I. M., Gallicchio, S. N., Graham, S. L., Selnick, H. G., Vacca, J. P., Kane, S. A., Pharmacological Properties of MK-3207, a Potent and Orally Active Calcitonin Gene-Related Peptide Receptor Antagonist. *Journal of Pharmacology and Experimental Therapeutics* **2010,** *333* (1), 152-160.
54. Gnanamony, M., Gondi, C. S., Chemoresistance in pancreatic cancer: Emerging concepts. *Oncology Letters* **2017,** *13* (4), 2507-2513.
55. Bhardwaj, A., Srivastava, S. K., Singh, S., Tyagi, N., Arora, S., Carter, J. E., Khushman, M., Singh, A. P., MYB Promotes Desmoplasia in Pancreatic Cancer through Direct Transcriptional Up-regulation and Cooperative Action of Sonic Hedgehog and Adrenomedullin. *Journal of Biological Chemistry* **2016,** *291* (31), 16263-16270.
56. Tahir, S. A., Yang, G., Ebara, S., Timme, T. L., Satoh, T., Li, L. K., Goltsov, A., Ittmann, M., Morrisett, J. D., Thompson, T. C., Secreted caveolin-1 stimulates cell survival/clonal growth and contributes to metastasis in androgen-insensitive prostate cancer. *Cancer Research* **2001,** *61* (10), 3882-3885.

Supporting Information

The Supporting Information is available as emailed electronic files in PDF format free of charge by request to t.skerry@sheffield.ac.uk

Supplementary chemistry: Chemical synthesis details, structures for screened compounds and modelling approach and supplemental biology: supplementary figures and supplementary tables.

Acknowledgments

We would like to thank the following for their assistance with these studies:

Prostate Cancer UK (Grant PA12-12), Wellcome Trust (Grants 104046/Z/14/1 and 205291/Z/16/Z) and the University of Sheffield for funding support for target validation, drug discovery research and proof of concept studies respectively,

Drs Richard Seabrook, Alan Naylor, Graham Showell and Georgios Trichas for support and advice during the research,

Drs Zaixu Xu and Genfu Chen of Wuxi AppTec for chemical synthesis and ADME studies respectively.

The reviewers of this article, whose constructive comments improved the clarity and focus of our original manuscript.

Author Contributions

P. A., A. B. A. J., J.-O. Z., M. J. T., K. R. G., P. A. G., J. E. J. M., R. A. P., P. B., P. J. B., N. W., T. M. S., J. P. A. H. and G. O. R. designed research; P. A., A. B. A. J., J.-O. Z., J. E. J. M., N. W., A. P. S., K. J. A. B., J. L. H. and J. I. W. performed research; J.-O. Z., P. B., and P. J. B. contributed new reagents/analytic tools; P. A., A. B. A. J., J.-O. Z., M. J. T., K. R. G., P. A. G., J. E. J. M., R. A. P., P. B., P. J. B., N. W., A. P. S., K. J. A. B., and J. I. W., T. M. S., J. P. A. H. and G. O. R. analysed data; P. A., A. B. A. J., J.-O. Z., M. J. T., K. R. G., P. A. G., J. E. J. M., R. A. P., P. J. B., T. M. S., J. P. A. H. and G. O. R. wrote the manuscript

Conflict of interest

Results and reagents arising from this study are currently the subject of patent fillings. The University of Sheffield is exploring the possibility of commercializing AM2 Antagonists as therapeutics. If this occurs, Timothy M Skerry, Joseph P A Harrity, Gareth O Richards, Paris Avgoustou, Ameera BA Jailani, and Jean-Olivier Zirimwabagabo may benefit financially from stock or other rewards for invention. If the research is commercialized, the following may receive payment for work to be performed during the commercialization process: Matthew J Tozer, Karl R Gibson, Paul A Glossop, James EJ Mills, Roderick A Porter, Peter J Bungay.

For Table of Contents Use Only

Title: Discovery of a first-in-class selective small molecule antagonist against the Adrenomedullin-2 receptor

Paris Avgoustou[1^], Ameera B A Jailani[1^], Jean-Olivier Zirimwabagabo[2^], Matthew J Tozer[3], Karl R Gibson[4], Paul A Glossop[4], James EJ Mills[4], Roderick A Porter[5], Paul Blaney[6], Peter J Bungay[7], Ning Wang[1], Alice P Shaw[1], Kamilla J A Bigos[1], Joseph L Holmes[1], Jessica I Warrington[1], Timothy M Skerry[1ǂ*], Joseph PA Harrity[2ǂ] and Gareth O Richards[1ǂ].

^ ǂ These authors contributed equally to the work

*Correspondence to T M Skerry
Email: t.skerry@sheffield.ac.uk

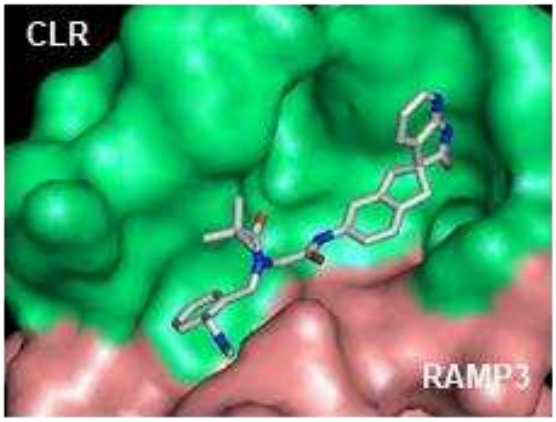

Compound 8 docked in AM_2R hybrid model

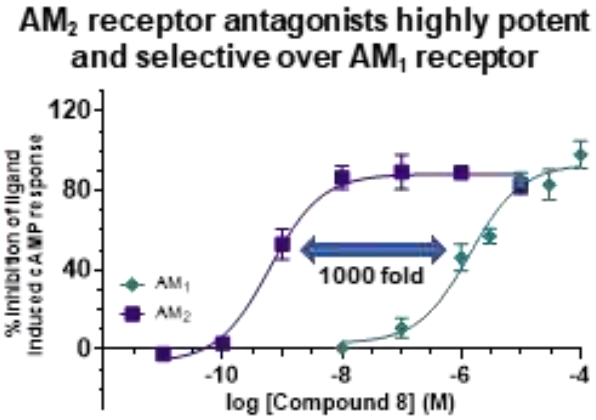

Brief synopsis: Graphic showing the docking of lead compound 8 in AM_2R hybrid model and its ability to inhibit AM induced cAMP response in both AM_1 and AM_2 overexpressing cells. Compound 8 is 1000-fold more potent on AM_2 receptor when compared to AM_1.